Journal of Plant Protection Research eISSN 1899-007X

ORIGINAL ARTICLE

Evaluating sensitivity of *Pyricularia oryzae* in Mekong Delta (Vietnam) to fungicides and effect of Ag/SiO_2 nanocomposites on chemical resistance isolates

Vo Thi Ngoc Ha*, Bui Quang Bao, Ngo Van Ngoi

Plant Protection, Nong Lam University Ho Chi Minh City, Ho CHi Minh, Viet Nam

Vol. 65, No. 3: 353–366, 2025

DOI: 10.24425/jppr.2025.155785

Received: September 17, 2024
Accepted: November 04, 2024
Online publication: September 17, 2025

*Corresponding address:
ha.vothingoc@hcmuaf.edu.vn

Responsible Editor:
Iwona Adamska

Abstract

Solving the fungicide resistance of the rice blast fungus *Pyricularia oryzae* (*P. oryzae*) is essential for rice production in the Mekong Delta region of Vietnam. Thus, this study aimed to investigate fungicide resistance and evaluate Ag/SiO_2 nanocomposites for controlling the chemical resistance of *P. oryzae*. Here, a total of 30 *P. oryzae* isolates was collected, and most of the isolates exhibited conidia with pyriform and short pyriform. The sensitivity in *vitro* of all isolates was measured against those three chemicals via the poisoning method. Furthermore, the EC50 and the resistance factor (RF) were evaluated for 12 days after inoculation. The obtained results revealed that all of the *P. oryzae* isolates were sensitive to tricyclazole; to chlorothalonil, 67% of them were sensitive, while the rest 33% were medium-sensitive. To azoxystrobin, 17% of them were sensitive, 57% were medium--sensitive, 23% were resistant, and the rest, 3%, were highly resistant. Subsequently, the antifungal activity of the Ag/SiO_2 nanocomposites against two *P. oryzae* resistance isolates (labeled TM4 and TAT2) was determined. Interestingly, Ag/SiO_2 nanocomposites exhibited a 100% inhibition effect for mycelial growth of TM4 and TAT2 isolates at a concentration of 60 $\mu g \cdot ml^{-1}$ because Ag/SiO_2 nanocomposites can activate the hyphae of *P. oryzae* to lose their typical structure (breaking filaments and damaging cell wall integrity). Overall, this study confirms the resistance of *P. oryzae* isolates to azoxystrobin and chlorothalonil and also highlights the potential of Ag/SiO_2 as an alternative solution to control blast rice disease.

Keywords: Ag/SiO_2, blast rice disease, fungicide resistance, nanocomposites, *Pyricularia oryzae*

Introduction

Rice is the main food crop of Vietnam, and agricultural development aims to ensure the food security of many rice-dependent countries. Vietnam is one of the world's largest rice producers and the second-largest rice exporter in the world, with an average production output in 2022 year of 42,672,338.69 tons. In an attempt to increase yield and quality of rice production one of the critical challenges for rice production to increase yield and quality is rice blast disease caused by *Pyricularia oryzae*, resulting in yield losses of up to 80% in susceptible varieties (Nalley *et al.* 2016; FAOSTAT 2024). The use of resistant varieties for limiting the disease effect has increasingly lost its advantages due to climate change. The pathogen quickly evolves to overcome plant resistance (Cai *et al.* 2021). The practical effectiveness of biocontrol methods which are based on plant extracts and biocontrol agents have limited in vitro studies, and is often unstable (Wiraswati *et al.* 2019). Consequently, fungicides have emerged as a crucial strategy in managing and mitigating the impact of rice blast disease.

Over 200 active ingredients have been allowed for blast rice control in Vietnam, mainly tricyclazole, azoxystrobin, isoprothiolane, and chlorothalonil

(LPAU&LPBU in Vietnam, 2023). The vast field sizes, along with potentially substantial economic losses, drive farmers to follow fungicide-spraying calendars, regardless of disease presence, promoting the emergence of fungicide-resistant populations (Kunova *et al.* 2014; D'Ávila *et al.* 2021). Pathogenic *P. oryzae* populations worldwide have been recorded to be resistant to azoxystrobin (Hirooka and Ishii 2013; Kunova *et al.* 2014; D'Ávila *et al.* 2021), carbendazim (Chuan-qing *et al.* 2004), and triazoles (Fang *et al.* 2009; Dorigan *et al.* 2019). Furthermore, a slight reduction in sensitivity to tricyclazole among the population in China and evidence that *P. oryzae* isolate is adapting to fungicide Bim® 750 BR (tricyclazole – 250 g · kg^{-1}) have been recorded (Chuan-qing *et al.* 2004; Bezerra *et al.* 2021). Besides diminishing the effectiveness of chemical treatments, the development of resistance in *P. oryzae* pathogens to fungicides has led to the need for higher doses or more frequent applications. As a result, there is growing public concern regarding fungicides' toxicity and subsequent effects. Numerous active ingredients in fungicides are being banned for the sake of safety, which is why, farmers and researchers are looking for alternative replacements.

Nanoparticles have demonstrated substantial efficacy in controlling a broad spectrum of pests (Okey-Onyesolu *et al.* 2021; Wang *et al.* 2021; Khan *et al.* 2022) and could play an important role in solving the problem of developing resistant pathogens. Silver nanoparticles (AgNPs) are one of the most abundant nanomaterials and have created great interest in agriculture due to their biocidal activity (Al-Zubaidi *et al.* 2019). By interrupting electron transport and disrupting cellular metabolism, AgNPs could attack many biological organelles, including the structure of the cell membrane (Guo *et al.* 2019). In addition, AgNPs damage DNA, inhibit protein synthesis related to ATP production, and inhibit cell proliferation (Akter *et al.* 2018). The biocidal activity of AgNPs is mainly determined by their size, surface properties, and the concentration used. In order to optimize the AgNPs properties and modeling of the biological activity, different stabilizing agents such as silica (SiO_2) and carboxyl methyl cellulose (CMC) were added during the AgNPs synthesis process. SiO_2 acts as a protective barrier to stop silver particles from agglomerating and stabilize the formation of AgNPs (Park *et al.* 2017). Meanwhile, CMC stabilizes the colloidal system and induces the oxidative dissolution of AgNPs, which causes the release of silver ions that interact with biomolecules within the cell, such as nucleic acids, and cell wall components (Rangelova *et al.* 2014; Prema *et al.* 2017; Salem *et al.* 2022). Moreover, for Ag/SiO_2, biologically active stabilizers can intensify the penetration of AgNPs through biological membranes and facilitate their accumulation in cell organelles.

There are studies on the antifungal activity of Ag/SiO_2 against *Fusarium oxysporium* and *Rhizoctonia solani* (Nguyen *et al.* 2016), *Aspergillus flavus* (Tran *et al.* 2023), *Botrytis cinerea* (Baka and El-Zahed 2022). However, very little data is available on the effect of Ag/SiO_2 against *P. oryzae* (rice blast fungus). Therefore, this study aimed to (1) collect the fungus causing rice blast disease in the main rice production area of the Mekong Delta (Vietnam), (2) examine the sensitivity of *P. oryzae* to tricyclazole, azoxystrobin, and chlorothalonil, and (3) develop Ag/SiO_2 nanocomposites via a chemical reduction of silver nitrate by $NaBH_4$ in the presence of CMC and evaluate the antifungal activity against two *P. oryzae* isolates that are resistant to chemical active ingredients. Overall, this study confirmed the presence of chemical resistant *P. oryzae* in the Mekong Delta (Vietnam) and suggested Ag/SiO_2 nanocomposite as a potential alternative solution for this problem.

Materials and Methods

Materials

Silver nitrate ($AgNO_3$, 99.0%, Xilong Scientific Co., Ltd., China), sodium borohydride ($NaBH_4$, 98.0%, Xilong Scientific Co., Ltd., China), hydrochloric acid (HCl, Xilong Scientific Co., Ltd., China), and carboxyl methyl cellulose (CMC, Xilong Scientific Co., Ltd., China, viscosity: 300–800 mPa s) were used. Agar powder (100%) was obtained from Hai Long Company (Vietnam). Rice husk silica (99.5%) was supplied by BSB Nanotechnology Joint Stock Company (Vietnam). Bi-distilled water was used throughout the experiments.

Technical-grade active ingredients (a.i.) including tricyclazole (95% a.i., Eastchem Co., Ltd., China), azoxystrobin (97% a.i., Eastchem Co., Ltd., China), and chlorothalonil (98% a.i., Shandong Weifang Rainbow Co., Ltd., China) were prepared by dissolving 0.5 g of powdered fungicide active ingredients with 99.6% acetone and adding distilled water to reach a volume of 100 ml. Then, the stock solution of each active ingredient was collected to a concentration of 5000 μg · ml^{-1}. The stock solutions were stored at 4°C in darkness and prepared within 2 weeks before the experiments.

Isolation of *Pyricularia oryzae*

Rice leaf samples showing typical blast symptoms were collected from rice variety IR504504 in different locations in the Mekong Delta regions of Vietnam in 2022 and 2023, under good weather conditions and from untreated rice fields. Samples were collected from

fields that had previously been reported to have rice blast disease and where chemical pesticides were regularly used for its control. The diseased samples were used for pathogen isolation in 48 hours. The place and time of rice blast sample collection for *P. oryzae* isolation are presented in Table 1.

Pyricularia oryzae were isolated using a single spore technique as described by Mew and Gonzales (2002). The collected samples were sterilized and incubated on moist filter paper in a Petri dish for 24 h and slightly scanned on aqueous agar medium (i.e., water agar or WA; consisting of 20 g agar in 1 l of distilled water). After that, a single spore was observed under a microscope and transported to potato dextrose agar (PDA – 200 g of potato, 20 g of agar, 20 g of D-glucose, and 1 l of distilled water) using a pipet (200 µl). The Petri dish was cultured at 26 ± 2°C for 7 days; the fungi colony was then transported to oatmeal medium (OMA – 50 g of powdered pulses, 20 g of agar, 20 g of glucose, and 1 l of distilled water) and kept at 26 ± 2°C to trigger the formation of conidia. Finally, these cultures of all single isolates carrying mycelia and conidia were stored at –20°C in sterile glass vials after necessary drying. The color of fungal colonies, melanin formation, growth, mycelium morphology, and morphology of conidia of each fungal isolate were observed (please see the process flow in Fig. 1A).

Sensitivity of *Pyricularia oryzae* populations to tricyclazole, chlorothalonil, and azoxystrobin active ingredients

A total of 30 *P. oryzae* isolates was used to determine the sensitivity to tricyclazole, chlorothalonil, and azoxystrobin (active ingredients) using the poisoned food method (Balouiri *et al.* 2016). The autoclaved PDA samples were amended with each active ingredient to obtain concentrations of tricyclazole: ca. 20, 40, 60, 80, 100, and 140 µg · ml^{-1}, those of chlorothalonil: ca. 0.5, 2, 5, 15, and 30 µg · ml^{-1}, and those of azoxystrobin:

Table 1. Place and time of blast rice sample collection for *Pyricularia oryzae* isolation

Isolates	Place of collection	Time	Isolates	Place of collection	Time	Isolates	Place of collection	Time
BL1	10°37′22.8″N 106°32′14.3″E	2023	TAT1	10°38′56.5″N 105°46′38.0″E	2023	TM1	10°32′42.9″N 105°54′18.9″E	2023
BL2			TAT2			TM2		
BL3			TAT3			TM3		
BL4			TAT4			TM4		
TTH1	10°36′54.1″N 106°25′46.1″E	2023	CL1	10°39′24.4″N 105°40′24.6″E	2023	TT1	10°30′30.7″N 104°52′17.7″E	2022
TTH2			CL2			TT2		
TTH3			CL3			TT3		
TTH4			CL4			TB1	10°34′26.6″N 104°55′40.8″E	2022
GT1	10°28′20″N 104°41′2″E	2022	TS1	10°16′13.4″N 105°07′43.7″E	2022	TB3		
GT2			TS2			TB4		

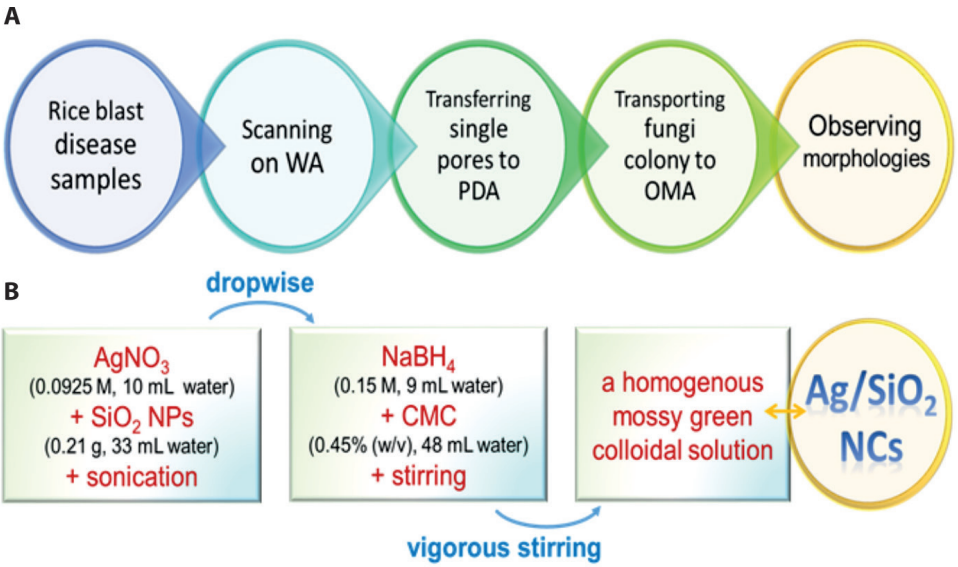

Fig. 1. A – schematic isolation process of *Pyricularia oryzae*; B – synthesis process of Ag/SiO_2 nanocomposites

ca. 0.01, 0.1, 0.5, 2, and 5 μg · ml^{-1}. An inverted 5 mm diameter mycelial plug (cut from the margin of a 7-day-old colony with a cork borer) was inoculated on the previously described PDA sample, and treatment. The control was made by adding an equal amount of distilled water (solvent) without fungicide was used The experiments were performed using a completely randomized design with four replicates. The plates were incubated at 28 ± 2°C for 12 days in the dark, and the diameter of mycelial growth was measured and processed using Microsoft Excel 2010. The mycelial growth inhibition rate (MGIR %) was calculated by Equation 1. Statistical analyses were conducted using one-way ANOVA with Duncan's multiple range test ($p < 0.01$) to determine the significant difference by SAS 9.1 software. To determine the EC50 value for each fungicide, the MGIR was regressed against log10 [fungicide]. EC50 was determined by solving the regression equation for log10 [fungicide] at MGIR 50% (Song *et al.* 2022).

$$\text{MGIR} = \frac{(1 - \text{diameter of the treatment})}{\text{diameter of the control}} \times 100\%. \quad \text{Eq. (1)}$$

Fungal isolates were then divided into groups based on the resistance coefficient – resistance factor (RF) (Gouot 1988) for all tested active ingredient fungicides. In this study, the isolates with the lowest EC50 for each a.i. were considered sensitive samples for those a.i. and used for observing the sensitivity of the rest of the *P. oryzae* isolates. The resistance factor (RF) was expressed as the ratio of the EC50 and the lowest EC50 among the *P. oryzae* isolates. Fungal isolates were classified into: the susceptible group if RF < 3, the medium resistant group if RF = 3÷20, the resistant group if RF = 20÷100, and the highly resistant group if RF > 100.

Synthesis of Ag/SiO_2 nanocomposites samples and their characterization

The Ag/SiO_2 colloidal nanocomposites (NCs) were synthesized via a chemical reduction of silver nitrate by $NaBH_4$ in the presence of CMC. Their synthesis route and detailed measured methods were previously described by Pham *et al.* (2021). Please see Figure 1B. Scanning electron microscopy (SEM, Hitachi S-4800) and transmission electron microscopy (TEM, JEOL, JEM-1400, 120 keV) were used to record the Ag/SiO_2 NCs' micrographs and determine the Ag NPs' morphology and size distribution. A Nanoparticle Analyzer (HORIBA, SZ-100) was used to measure the hydrodynamic size (DLS) and the zeta potential (surface charge) of Ag/SiO_2 NCs.

Evaluation of the antifungal activity of nanomaterials against *Pyricularia oryzae*

The experiment was carried out using the poisoned food method, as described in section 2.3. The Ag/SiO_2 stock solution was adjusted to pH = 6.5–7.0 with the HCl solution (1M) before adding to the PDA medium. To determine the sensitivity of *P. oryzae* to Ag/SiO_2 NCs, a series of concentrations of 15, 30, 45, 60, 75, and 90 μg · ml^{-1} was used to calculate the effective concentration of Ag/SiO_2 NCs inhibiting colony growth by 50% (EC50) values. In addition, the stabilization at a CMC concentration of 90 μg · ml^{-1}, and H2O was used as the control. Mycelial plugs of the TM4 and TAT2 strains were inoculated on PDA plates supplemented with a series of the above concentrations. Two-factor experiments were performed using a completely randomized design with factor A as a *P. oryzae* isolate and factor B as a concentration of Ag/SiO_2, four replicates of each variant, and one replicate of one Petri dish. The diameter of mycelial growth was determined and processed using Microsoft Excel 2010, and the mycelial growth inhibition (MGIR %) was investigated by Equation 1. Statistical analyses were conducted using one-way ANOVA with Duncan's multiple range test ($p < 0.01$) to determine the significant difference by SAS 9.1 software.

Results

Isolation and characterization of *Pyricularia oryzae*

In this study, 30 *P. oryzae* isolates were isolated using the single spore method. The morphological characteristics of 30 rice blast isolates were examined. Fungal filaments on PDA plates were observed after 12 days and transferred to OMA to stimulate conidia formation and to observe conidia shape under a microscope. The colony had thin gray-white mycelium, the surface of the mycelium was quite rough, and the margin of the fungal colony was clear; flat or fluffy filaments and filament density were observed for filamentous patterns. Melanim pigment (black pigment) was in the center and became faded towards the outside. Here, Figure 2 records the morphological characteristics of conidia forms of *P. oryzae*. Most of the isolates had conidia with a pyriform shape and short pyriform conidia (isolates CL1, TTH1, TTH2, TTH3, TTH4, TB1 and TB3); the conidia of all *P. oryzae* isolates had 2 septa. The colony characteristics, melanin pigment, and shape of conidia are essential factors for *P. oryzae* identification.

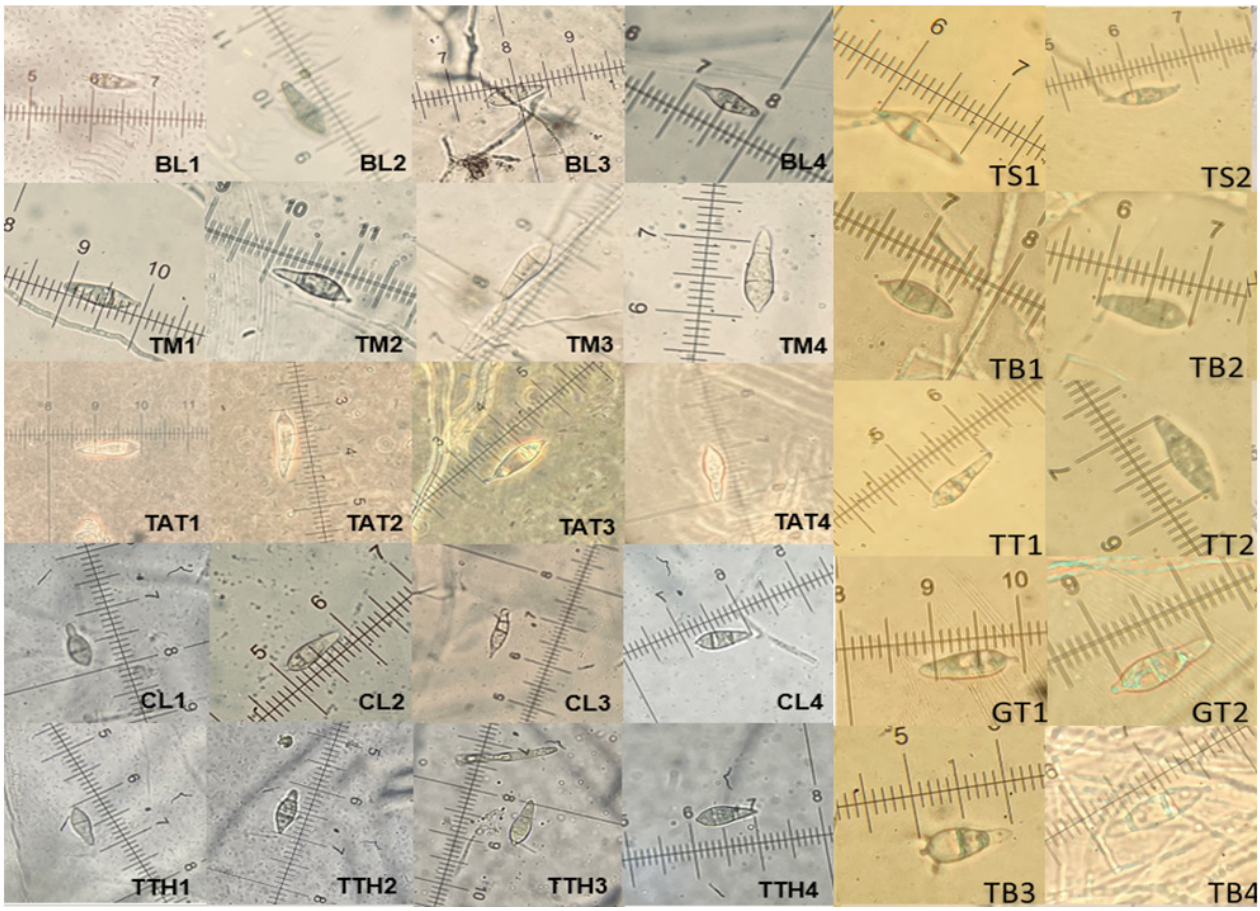

Fig. 2. Conidia morphologies of 30 *Pyricularia oryzae* isolates

Sensitivity of *Pyricularia oryzae* populations to tricyclazole, chlorothalonil, and azoxystrobin

The investigated concentrations of three chemical active ingredients were suitable for examining the resistance of *P. oryzae*. The mycelial growth inhibition rate of tricyclazole, chlorothalonil, and azoxystrobin were recorded in Table 2. The mycelial growth of 63% *P. oryzae* isolates was completely inhibited on PDA media, and amended with tricyclazole at 140 μg · ml^{-1} while the remaining had weak growth. The lowest MGIR was observed in *P. oryzae* isolates BL4 and TAT2, which, respectively, was 79.5% and 73.1% at 140 μg · ml^{-1} of tricyclazole; and the difference was significant at $p \leq 0.01$ (Table 2).

An effect on the radial mycelial growth of all *P. oryzae* isolates was observed in all used concentrations of chlorothalonil. In the case of 30 μg · ml^{-1} concentration of chlorothalonil, there was no radial mycelial growth (i.e., 100% mycelial growth inhibition) in plates with *P. oryzae* isolate TB4. *P. oryzae* isolates TTH1, TM4, TAT2, TAT3, CL2, and TB1 showed the lowest MGIR at all chlorothalonil concentrations. The difference was significant at $p \leq 0.01$ (Table 2).

Azoxystrobin completely inhibited the mycelial growth of *P. oryzae* isolates BL2, TT3, and TB1 (MGIR was 100%) at a concentration of 5 μg · ml^{-1}. The lowest MGIR at 5 μg · ml^{-1} of azoxystrobin was 52.0% observed in *P. oryzae* isolate TM4, followed by *P. oryzae* isolates TAT2, TAT3, and TT2 with MGRI 60.7%, 62.2% and 62.8%, respectively. The difference was significant at $p \leq 0.01$ (Table 2).

The linear regression equation for EC50 determination of each isolate was established with a strong positive correlation, R^2 value ≥ 0.9410 for tricyclazole, R^2 value ≥ 0.8373 for chlorothalonil and R^2 value ≥ 0.7831 for azoxystrobin (Sup. Table).

The investigated concentrations for calculating EC50 of tricyclazole, chlorothalonil, and azoxystrobin were varied according to their active mechanisms. Although the linear regression equations were recorded using the mycelial growth inhibition rate, the EC50 of each chemical active ingredient for each isolate could finally be determined, as shown in Table 3. In this study, the isolates with the lowest EC50 were considered sensitive samples for observing the sensitivity of *P. oryzae* collection. The RF value of the rest of the studied fungal isolates was calculated by dividing the EC50 to the lowest EC50 among the fungal isolates.

Table 2. Mycelial growth inhibition rate of tricyclazole, chlorothalonil, and azoxystrobin at different concentrations

P. oryzae isolate	MGIR of tricyclazole [%]*					MGIR of chlorothalonil [%]*					MGIR of tricyclazole [%]*				
	20 µg · ml^{-1}	40 µg · ml^{-1}	80 µg · ml^{-1}	100 µg · ml^{-1}	140 µg · ml^{-1}	0,5 µg · ml^{-1}	2 µg · ml^{-1}	5 µg · ml^{-1}	15 µg · ml^{-1}	30 µg · ml^{-1}	0.01 µg · ml^{-1}	0.1 µg · ml^{-1}	0.5 µg · ml^{-1}	2.0 µg · ml^{-1}	5.0 µg · ml–1
BL1	15.0 a–d	30.5 a–e	67.9ab	77.0 c–f	96.9a	21.4 b–d	31.4 d–f	38.9 c–f	45.7 kl	61.3 i–l	37.8 a	57.0 a	67.8 ab	80.5 b	87.3 cd
BL2	18.7 a–c	26.9 b–e	47.7h–i	69.9 e–h	100.0a	24.9 b	31.5 d–f	41.5 c–e	62.9 b–d	86.4 b	37.2 a	53.4 a–c	67.5 ab	83.7 ab	100.0 a
BL3	3.2 g–i	36.7 ab	55.0d–f	95.3 a	100.0a	13.1 f–i	24.9 h–j	32.5 g–j	43.5 lm	62.1 h–l	37.3 a	46.7 c–f	60.8 c–e	67.8 c–e	85.6 c–e
BL4	1.9 hi	11.7 i–k	29.0n	45,7 l–n	79.5d	13.1 f–i	20.1 i–l	26.4 j–l	51.1 g–j	60.6 j–m	19.1 d–h	51.4 a–d	69.0 a	86.8 a	94.1 b
TTH1	2.8 g–i	6.7 k	20.6o	37.8 n	80.7cd	8.8 i	21.5 h–j	28.2 j–l	47.0 i–l	58.3 k–n	18.9 d–h	33.8 i–j	45.4 h	60.0 f–h	68.8 i–l
TTH2	6.5 d–i	31.8 a–d	49.8f–i	59.2 h–k	100.0a	21.3 b–d	29.0 e–g	38.8 c–f	56.9 ef	71.8 c–e	31.8 ab	53.8 ab	64.0 bc	71.7 cc	78.1 e–j
TTH3	21.7 a	33.7 a–c	61.4cd	74.9 c–g	87.8b	23.7 b	34.2 c–e	41.8 cd	67.6 a	75.6 c	7.6 k	27.4 l	39.3 i	57.7 gh	74.4 g–j
TTH4	11.6 a–f	26.2 b–e	63.0bc	74.5 c–g	100.0a	21.0 b–d	29.6 e–g	32.4 h–i	43.0 lm	60.8 j–m	14.3 f–j	27.3 l	35.7 i	44.9 kl	76.4 f–j
TM1	2.6 hi	13.7 h–k	29.2n	42.7 mn	87.5b	10.0 hi	17.9 kl	31.4 j–l	45.7 kl	65.3 g–h	24.8 b–d	51.3 a–d	61.1 cd	68.4 c–e	75.8 f–j
TM2	3.2 hi	10.4 i–k	23.0o	49.3 k–l	100.0a	19.8 b–d	30.6 d–f	38.2 d–h	47.6 i–l	71.7 de	29.7 bc	47.2 b–f	57.9 d–f	68.6 c–e	81.8 c–g
TM3	3.3 g–i	10.3 i–k	30,9mn	56.7 j–l	100.0a	15.8 d–g	24.8 g–i	34.8 e–i	46.3 j–l	67.6 fg	22.6 c–f	40.9 f–h	55.2 f	63.1 e–g	76.5 f–j
TM4	2.7 hi	7.3 jk	30.0n	49.5 k–l	80.3cd	15.7 d–g	22.9 h–j	27.8 l	39.3 m	58.5 k–n	8.8 jk	17.0 mn	28.8 j	39.6 l	52.0 m
TAT1	6.9 d–i	22.2 d–g	54.3e–g	68.8 e–i	100.0a	14.3 f–i	22.7 h–l	28.4 kl	50.5 i–l	67.7f g	20.5 d–h	50.6 a–c	61.5 cd	66.8 c–e	73.4 g–j
TAT2	2.2 hi	7.8 jk	20.6o	35.8 n	73.1d	11.1 g–i	16.5 l	25.6 l	39.3 m	55.8 n	8.6 j–k	15.3 n	30.5 j	45.7 jk	60.7l m
TAT3	4.5 f–i	11 i–k	37.1k–m	51.0 k–l	88.2b	12.1 g–i	18.4 j–l	27.7 j–l	44.8 l	56.5 mn	12.8 g–k	20.3 m	29.1 j	50.9 ij	62.2 kl
TAT4	21.5 a	35.7 ab	56.7c–f	81.5 b–d	100.0a	13.8 e–h	31.0 d–f	39.0 c–f	48.0 i–l	67.0 fg	13.4 g–k	25.8 l	37.1 i	50.5 i–kj	64.0 kl
CL1	6.9 d–i	14.3 g–j	33.2l–n	50.6 k–l	86.1bc	18.9 b–f	24.7 g–i	33.1 f–i	44.8 l	65.6 gh	22.8 b–e	49.0 b–e	55.3 f	63.8 e–g	78.3 e–i
CL2	2.7 hi	11.6 i–k	34.2l–n	58.2 i–k	89.3b	16.9 c–f	21.5 h–j	29.7 j–l	43.0 lm	58.9 k–n	18.4 d–h	45.8 d–f	55.9 ef	70.8 cd	79.3 e–h
CL3	9.0 c–h	32.4 a–d	69.8 a	85.7 b	100.0 a	18.3 b–f	25.9 f–h	30.5 j–l	50.3 i–j	60.7 j–m	16.0 e–i	45.5 h–j	38.0 i	65.6 d–f	72.6 g–j
CL4	10.5 b–g	22.3 d–g	47.9 g–j	69.6 e–h	100.0 a	22.8 bc	32.4 de	38.6 c–g	47.2 i–l	60.5 j–m	12.6 h–k	28.0 kl	46.3 h	59.0 gh	78.2 e–j
TS1	7.8 c–h	12.3 i–k	43.6 i–j	78.5 b–e	100.0 a	18.4 b–f	31.9 de	42.3 cd	57.6 d–f	64.0 g–j	20.8 c–g	51.5 a–d	55.0 f	63.0 e–g	70.8 h–k
TS2	7.6 d–i	31.5 a–e	41.4 jk	57.9 h–k	87.1 b	35.4 a	41.4 ab	49.2 ab	60.1 c–f	70.5 ef	25.7 b–d	40.3 f–h	53.1 fg	59.5 gh	87.4 c
TT1	7.4 d–i	23.7 c–f	54.5 e–g	71.1 e–g	100.0 a	20.2 b–d	41.7 ab	49.8 ab	55.7 e–h	73.3 c–e	22.3 c–f	48.2 b–d	55.7 ef	67.3 c–e	82.4 c–g
TT2	14.0 a–e	31.4 a–e	42.5 jk	59.0 h–k	100.0 a	31.4 a	36.1 b–d	45.0 bc	55.4 e–g	70.3 ef	10.8 i–k	46.4 c–f	55.0 f	62.8 e–g	62.8 j–l
TT3	19.0 ab	35.1 ab	53.8 e–h	83.6 bc	100.0 a	30.2 a	38.8 a–c	53.4 ab	62.2 b–d	74.7 cd	21.9 c–f	43.3 e–g	57.3 ef	81.5 b	100.0 a
GT1	6.2 e–i	21.0 f–h	41.5 jk	73.0 d–g	100.0 a	18.0 b–f	33.2 c–e	41.8 cd	52.0 g–i	62.6 h–j	19.2 d–h	31.5 j–l	44.5 h	54.9 hi	78.1 e–j
GT2	1.6 i	24.2 c–e	42.4 jk	65.7 g–j	100.0 a	20.2 b–d	26.0 f–h	49.2 ab	64.2 a–c	100.0 a	20.7 c–g	31.7 j–l	44.6 h	58.7 ghg	84.3 c–f
TB1	3.6 g–i	15.5 f–i	33.7 l–n	59.0 h–k	100.0 a	21.4 b–d	29.0 e–g	38.5 c–g	50.7 h–k	57.8 l–n	9.8 i–k	40.3 f–h	52.9 fg	66.6 c–e	100.0 a
TB3	3.4 g–i	8.2 i–k	38.5 kl	66.8 f–j	100.0 a	32.0 a	44.5 a	54.7 a	66.6 ab	75.5 c	23.0 b–e	41.2 f–h	48.6 gh	55.6 hi	76.6 f–j
TB4	3.0 hi	38.0 a	60.2 c–e	68.6 e–i	100.0 a	22.2 bc	36.9 c–e	44.6 cd	62.7 c–e	100.0 a	13.1	39.1 g–i	48.5 gh	65.6 d–f	81.3 c–g
CV (%)	23.7	10.3	4.1	5.0	2.8	6.8	4.6	4.0	2.6	1.8	9.3	4.1	2.9	2.8	3.8
P	0.0001	0.0001	0.0001	0.0001	0.0001	0.0001	0.0001	0.0001	0.0001	0.0001	0.0001	0.0001	0.0001	0.0001	0.0001

*the mean values (followed by a common letter) of 4 repeated experiments shown in each column did not significantly differ at $p \leq 0.01$

The lowest EC50 for tricyclazole was *P. oryzae* CL3 (55. μg · ml^{-1}), that for chlorothalonil was *P. oryzae* TB3 (5 μg · ml^{-1}), and that for azoxystrobin was *P. oryzae* BL1 (0.04 μg · ml^{-1}), as shown in Table 3.

In general, the RF of 30 *P. oryzae* isolates for each a.i. was varied in a wide range and higher with the azoxystrobin (RF ranging from 1.3 to 106.3) than with the tricyclazole (RF ranging from 1.1 to 2.1) and chlorothalonil (RF ranging from 1.3 to 4.5), as shown in Table 3. The rate of insensitivity to azoxystrobin among these 30 *P. oryzae* isolates was higher than to either tricyclazole or chlorothalonil. All of the *P. oryzae* isolates were sensitive to tricyclazole, but 67% of them were sensitive to chlorothalonil, and 33% of them were medium-sensitive. In addition, 17% of *P. oryzae* isolates were sensitive to azoxystrobin, while 57% were medium-sensitive, 23% were resistant, and 3% were highly resistant (Table 3 and Fig. 3).

The EC50 range for tricyclazole was quite broad and varied from 55.50 μg · ml^{-1} (isolate CL3) to 117.10 μg · ml^{-1} (isolate TAT2). Based on RF ≤ 2,1, all of the 30 *P. oryzae* isolates were sensitive to tricyclazole (Table 3, Fig. 3). The EC50 for chlorothalonil varied from 5.0 μg · ml^{-1} (isolate TB3) to 22.50 (isolate TAT2). Interestingly, the isolates collected from one place simultaneously showed different EC50 and levels of sensitivity to the chlorothalonil. Based on the RF results, 67% of isolates were sensitive to chlorothalonil (Fig. 3), from which all were collected in 2022, and half were collected in 2023. The remaining isolates of 2023 involved BL1, BL3, TTH1, TTH4, TM1, TM3, TM4, TAT2, TAT3 and CL1were medium sensitive (Table 3).

Table 3. Isolates, EC50, RF, and sensitivity classification of *Pyricularia oryzae*

Isolates	Tricyclazole			Chlorothalonil			Azoxystrobin		
	EC_{50}	RF	sensitivity	EC_{50}	RF	sensitivity	EC_{50}	RF	sensitivity
BL1	59.4	1.1	S	16.2	3.2	MR	0.04	1.0	S
BL2	78.5	1.4	S	8.9	1.8	S	0.05	1.3	S
BL3	58.5	1.1	S	17.5	3.5	MR	0.09	2.3	S
BL4	106.2	1.9	S	14.6	2.9	S	0.1	2.5	S
TTH1	114.4	2.1	S	16	3.2	MR	0.61	15.3	MR
TTH2	80.4	1.4	S	10.6	2.1	S	0.08	2.0	S
TTH3	63.3	1.1	S	7.4	1.5	S	1.34	33.5	R
TTH4	65.8	1.2	S	19.8	4.0	MR	2.21	55.3	R
TM1	104.8	1.9	S	16	3.2	MR	0.15	3.8	MR
TM2	103.8	1.9	S	14.7	2.9	S	0.14	3.5	MR
TM3	97.2	1.8	S	15.6	3.1	MR	0.28	7.0	MR
TM4	103.8	1.9	S	22.4	4.5	MR	4.25	106.3	HR
TAT1	75.2	1.4	S	14.6	2.9	S	0.19	4.8	MR
TAT2	117.1	2.1	S	22.5	4.5	MR	2.15	53.8	R
TAT3	97.8	1.8	S	18.1	3.6	MR	1.85	46.3	R
TAT4	61.5	1.1	S	13.6	2.7	S	1.73	43.3	R
CL1	98.6	1.8	S	17.3	3.5	MR	0.2	5.0	MR
CL2	95.3	1.7	S	6.8	1.4	S	0.22	5.5	MR
CL3	55.5	1.0	S	8.6	1.7	S	1.00	25.0	R
CL4	77.9	1.4	S	10	2.0	S	0.57	14.3	MR
TS1	79.8	1.4	S	9.4	1.9	S	0.25	6.3	MR
TS2	86.5	1.6	S	6.8	1.4	S	0.24	6.0	MR
TT1	73.5	1.3	S	8.6	1.7	S	0.19	4.8	MR
TT2	86.2	1.6	S	10	2.0	S	0.4	10.0	MR
TT3	66.8	1.2	S	6.4	1.3	S	0.5	12.5	MR
GT1	81.3	1.5	S	11.3	2.3	S	0.57	14.3	MR
GT2	82.8	1.5	S	8.3	1.7	S	1.2	30.0	R
TB1	93.8	1.7	S	13	2.6	S	0.25	6.3	MR
TB3	81.9	1.5	S	5	1.0	S	0.4	10.0	MR
TB4	66.2	1.2	S	8.7	1.7	S	0.36	9.0	MR

S – sensitive; MR – medium resistance; R – resistance; HR – high resistance

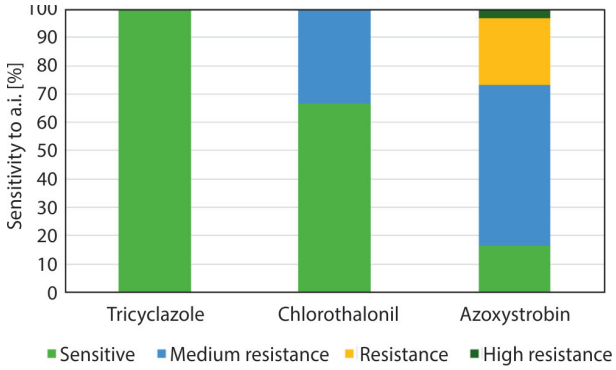

Fig. 3. The sensitivity classification of *Pyricularia oryzae* isolates to 3 chemical a.i.

With the azoxystrobin, the EC50 of 30 *P. oryzae* isolates varied from 0.04 μg · ml^{-1} (isolate BL1) to 4.25 μg · ml^{-1} (isolate TM4). The isolates BL1, BL2, BL3, BL4 and TTH2 were sensitive to azoxystrobin with the EC50 ≤ 0.1 μg · ml^{-1} and RF ≤ 2.5. Isolate TM4 had a high resistance to azoxystrobin with EC50 4.25 μg · ml^{-1} and RF 106.3. The *P. oryzae* isolates TTH3, TTH4, TAT2, TAT3, TAT4, CL3, and GT2 showed resistance, while the remaining isolates were considered medium resistant.

Synthesis of Ag/SiO_2 NCs and its antifungal activity against *Pyricularia oryzae in vitro*

Figure 4 shows the physico-chemical characteristics of Ag/SiO_2 NCs. Based on the SEM and TEM micrographs of the SiO_2 and Ag/SiO_2 samples (Fig. 4A–D), it was shown that the Ag/SiO_2 NCs exhibited a large amount of Ag NPs, which were tightly and uniformly dispersed on the silica surface. The average size of Ag NPs in the Ag/SiO_2 NCs was equal to 6.4 ± 0.1 nm.

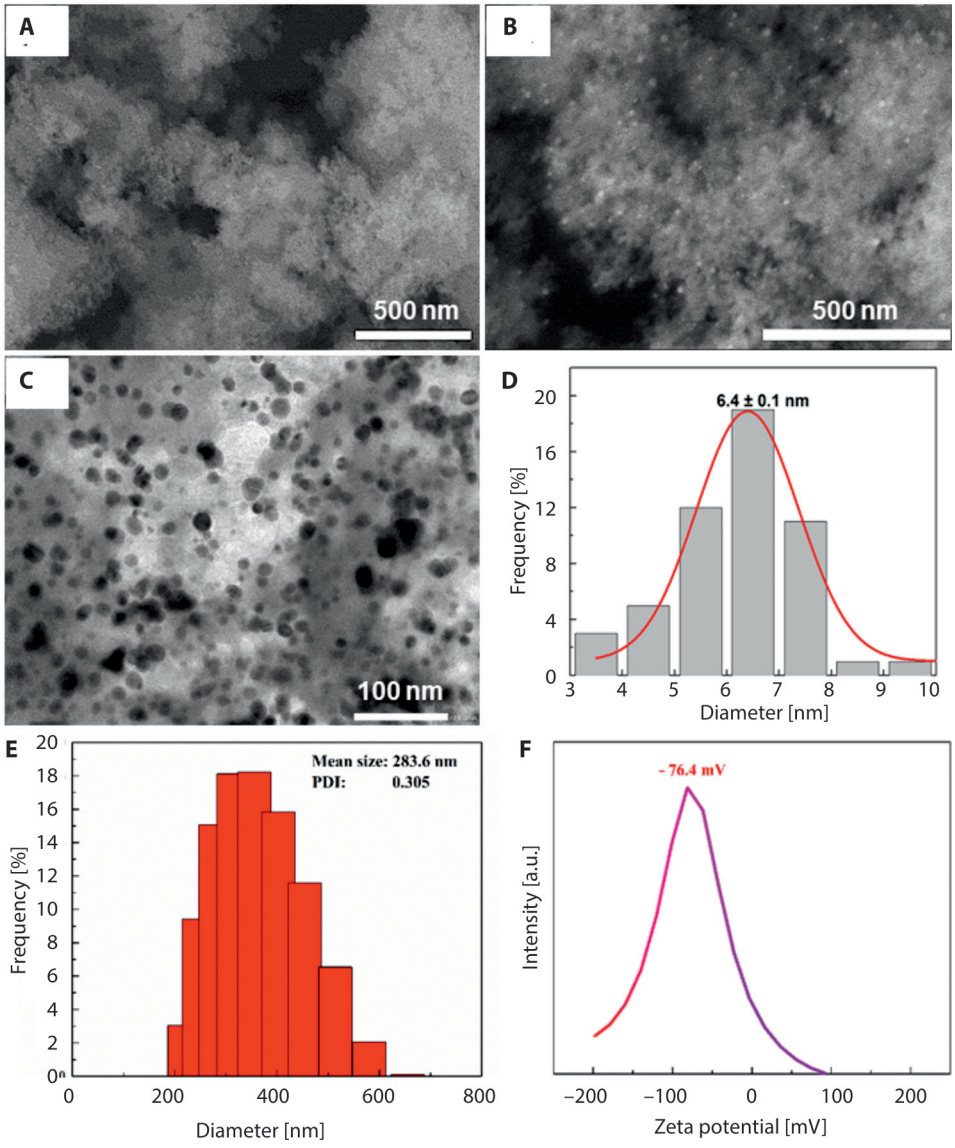

Fig. 4. A–B – SEM images of SiO_2 and Ag/SiO_2 NCs; C – TEM images of Ag/SiO_2 NCs; – particle size distribution of AgNPs; E – DLS result of Ag/SiO_2 NCs; F – zeta potential of Ag/SiO_2 NCs

The dynamic light scattering and zeta potential results revealed that Ag/SiO_2 NCs had a small particle size (mean diameter of 283.6 nm) and a negative surface charge (zeta potential of –76.4 mV), as displayed in Figure 4E–F.

Pyricularia oryzae fungus isolates TM4, and TAT2 fully covered the potato dextrose agar plate (control) 12 days after inoculation. As shown in Figure 5, 6 and Table 4, the CMC did not show any effect against *P. oryzae*, and the growth of both isolates TM4 and TAT2 at a CMC concentration of 90 µg · ml^{-1} for 12 days after inoculation (DAI) was the same as the control.

The results showed that $AgSiO_2$ NCs, especially at a concentration of 60 µg · ml^{-1} and higher, strongly limited the vegetative mycelium growth of both *P. oryzae* isolates. The colony diameter was always decreased compared to the control. The mycelial growth of *P. oryzae* isolates TM4 and TAT2 was significantly reduced with increasing concentrations of supplemented Ag/SiO_2 NCs and completely inhibited by Ag/SiO_2 NCs at concentrations ≥ 60 µg · ml^{-1}. In addition, at

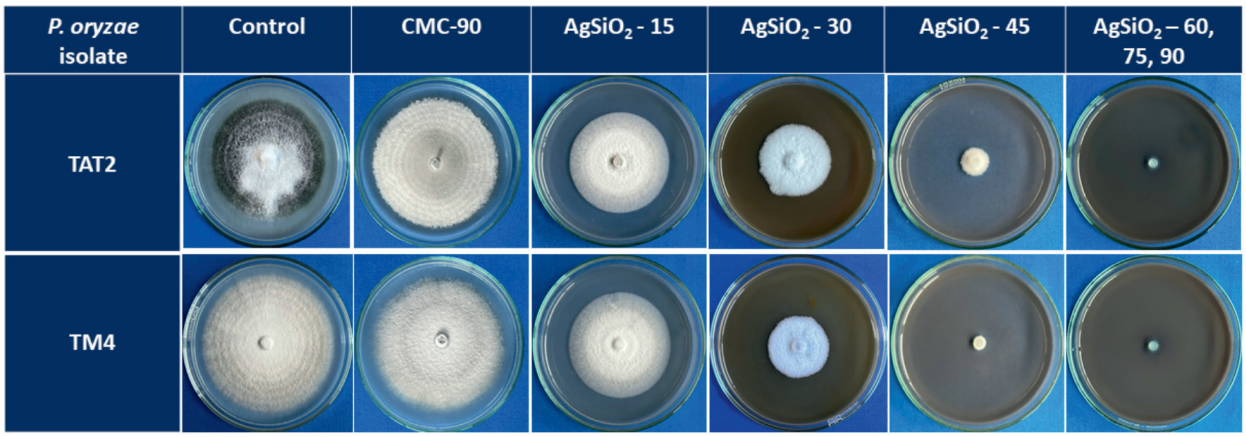

Fig. 5. Ag/SiO_2 NCs inhibited the mycelial growth of *Pyricularia oryzae* TAT2 and TM4 in a concentration-dependent manner. Here, the number after the component name is its concentration (µg · ml^{-1})

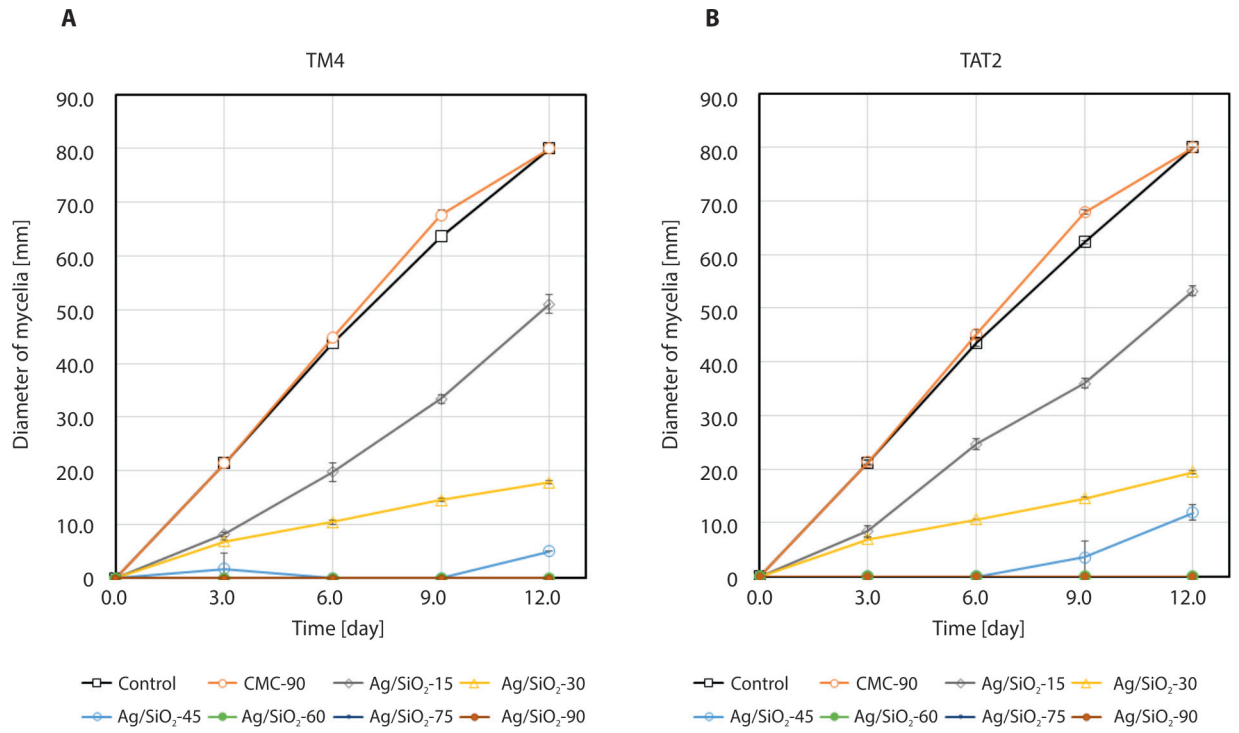

Fig. 6. Diameter of mycelia of the *Pyricularia oryzae* TM4 –A and TAT2 – B cultured on PDA amended with various concentrations of Ag/SiO_2 NCs

Table 4. Mycelial growth and mycelial growth inhibition rate of Ag/SiO_2 NCs on the 12th day after inoculation

P. oryzae isolate (A)		Mycelial growth [mm]*			Mycelial growth inhibition rate [%]*		
		TM4	TAT2	TB B	TM4	TAT2	average B
Control		80.00 a	80.00 a	80.00 A	-	-	
Concentration of Ag/SiO_2 NCs - (B)	15 µg · ml^{-1}	51.03 c	53.27 b	52.15 B	36.21	33.42	34.81 D
	30 µg · ml^{-1}	17.80 e	19.47 d	18.63 C	77.75	75.67	76.71 C
	45 µg · ml^{-1}	5.00 g	11.90 f	8.45 D	93.75	85.13	89.44 B
	60 µg · ml^{-1}	0.00 h	0.00 h	0.00 E	100.00	100.00	100.00 A
	75 µg · ml^{-1}	0.00 h	0.00 h	0.00 E	100.00	100.00	100.00 A
	90 µg · ml^{-1}	0.00 h	0.00 h	0.00 E	100.00	100.00	100.00 A
CMC	90 µg · ml^{-1}	80.00 a	80.00 a	80.00 A	0.00	0.00	0.00 E
Average A		30.40 B	32.69 A		66,78	63,69	
		CV (%) = 1.56; $Prob_A$ = 0.0001 $Prob_B$ = 0.0001; $Prob_{AB}$ = 0.0001			CV (%) = 0.82; $Prob_A$ = 1.0000 $Prob_B$ = 0.0001; $Prob_{AB}$ = 1.0000		

*the mean values (followed by a common letter) of 4 repeated experiments shown in each column did not significantly differ at $p \leq 0.01$

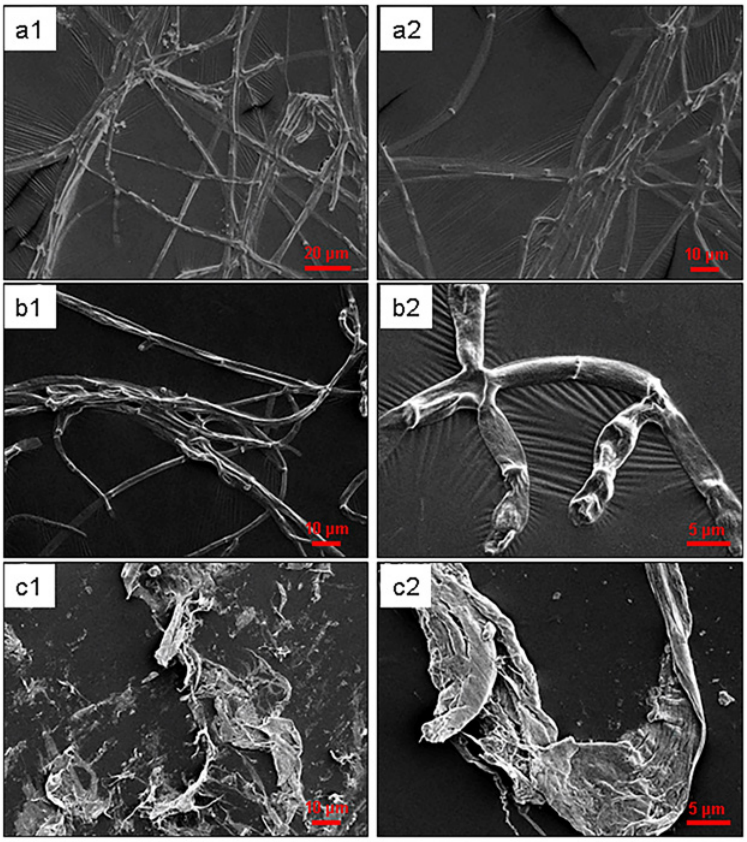

Fig. 7. The effect of Ag/SiO_2 NCs and chlorothalonil on hypha of *Pyricularia oryzae* isolates TM4 (a1, a2) with only the control, (b1, b2) with chlorothalonil treatment, and (c1, c2) with Ag/SiO_2 NCs treatment}

the same concentration of Ag/SiO_2 NCs, the mycelial growth of TM4 was significantly lower than that of TAT2. The mycelial growth inhibition rate (MGIR) was increased with the growth of Ag/SiO_2 NCs concentration and reached 93.75% and 85.13% for TM4 and TAT2, respectively, at the Ag/SiO_2 NCs concentration of 45 µg · ml^{-1}; the MGIR did not significantly differ between these isolates.

The EC50 of Ag/SiO_2 NCs for TM4 and TAT2 was 17.14 µg · ml^{-1} and 19.04 µg · ml^{-1}, respectively.

Visually, the intensity of melanin production was slightly decreased, especially from an Ag/SiO_2 NCs concentration of 45 $\mu g \cdot ml^{-1}$; the mycelia formed without melanin and turned white compared to the control. This indicated that despite inhibition of the mycelia growth of *P. oryzae*, the Ag/SiO_2 NCs could also affect melanin formation and the structure of hypha. To evaluate the effect of Ag/SiO_2 NCs on hypha, the SEM image of TM4 was taken at a concentration of EC50 values for Ag/SiO_2 NCs. The chemical a.i. 'chlorothalonil' was used to compare the impact of Ag/SiO_2 NCs and chemicals on *P. oryzae* mycelium.

Based on SEM results in Fig. 7, the net smooth surface of the hyphal structure was seen in the non-treated control samples of TM4, while the typical structure was not maintained when it was exposed to 17.14 $\mu g \cdot ml^{-1}$ of Ag/SiO_2 NCs and 22.4 $mg \cdot ml^{-1}$ of chlorothalonil. Control (non-treated) samples of TM4 showed nice filamentous tubular hyphae (Fig. 7a1, a2), while treated samples showed severely deformed hyphal structures and damage to the external morphology. The treated TM4 sample with chlorothalonil caused the hyphae of this fungal species to shrink compared to the control, with craters of different sizes (arrows) (Fig. 7b1, b2). While the Ag/SiO_2 NCs – treated sample lost its typical hyphal structure, the filaments were broken and arranged in patches. In some places, the hyphae sheath structure was broken into pieces (Fig. 7c1, c2), implicating damage to fungal cell wall integrity, and the formation of degenerative changes, including applanation and exfoliated flakes.

Discussion

Rice production in the Mekong Delta faces difficult challenges, including climate change, salinity intrusion, flooding, and the rapid adaptation of pests, including *P. oryzae*, which cause rice blast disease. Although planting blast-resistant rice cultivars significantly reduced blast rice disease, rice blast-resistant cultivars have become susceptible after planting for several years due to pathogenic variations in the *P. oryzae* populations. The application of fungicides is important in the management of rice blast disease in the field. However, there is a lack of information about the resistance of *P. oryzae* pathogen populations in the Mekong Delta, Vietnam, to existing pesticide-active ingredients involving azoxystrobin, tricyclazole, and chlorothalonil, which have been widely used to control rice blast for a long time (Froyd 1978; Balba 2007).

These factors motivated the research presented here, and for this, *P. oryzae* was collected from different places in the Mekong Delta. Although molecular methods using *ITS* or *TEF* sequences are preferred for identifying *P. oryzae*, this study employed a more traditional morphological approach for initial classification. However, by following the rigorous protocol for disease sample collection, single spore isolation, and UV-induced sporulation, the morphological characteristics of 30 rice blast isolates in this study involving colony characteristics, melanin pigment, and the shape of conidia were accurately presented for *P. oryzae,* and confirmed that all fungal isolates were indeed *P. oryzae* (Mew and Gonzales 2002; Longya *et al.* 2020).

The mycelial growth method was used to assess the sensitivity of *P. oryzae* collection to fungicides. The sensitivity of 30 *P. oryzae* isolates to azoxystrobin was lower than that to tricyclazole, and chlorothalonil. The same result was observed with the *P. oryzae* population collected by D'Ávila *et al.* (2021). Azoxystrobin is a broad-spectrum pesticide that is registered to control major diseases like rice blast (*P. oryzae*), dirty panicle or seed discoloration, sheath blight (*Rhizoctonia solani*), and brown spot (*Bipolaris oryzae*) in rice, as well as against various fungal diseases in many crops (Balba 2007; LPAU&LPBU in Vietnam 2023). As a result, azoxystrobin is intensively and repetitively used in rice fields, which has led to selection pressure for resistant populations of the rice blast fungus. On the other hand, azoxystrobin acts as a quinone outside inhibitor (QoI), targeting mitochondrial respiration. Resistance often arises from mutations in the target gene (cytochrome b), which can occur relatively easily, and reduce fungicide binding (Kim *et al.* 2008; D'Ávila *et al.* 2022).

In this study, the EC50 value of tricyclazole to control 50% mycelial growth of *P. oryzae* strains tended to be higher than in previous research. However, resistance to this a.i. was not found. Tricyclazole works by inhibiting melanin biosynthesis in *P. oryzae*. Melanin is critical for the pathogen's ability to penetrate rice plant cells by forming an appressorium-specialized structure. Due to this specific action, resistance requires mutations in the melanin pathway, which are complex and less likely to evolve easily under field conditions (Woloshuk 1980; Kunova and Cortesi 2013). In addition, genes involved in melanin synthesis, such as polyketide synthase, have a lower mutation rate and are tightly regulated. Mutations that disrupt melanin synthesis may also interfere with other critical functions, reducing the likelihood of viable resistant strains emerging. Moreover, mutations impacting melanin synthesis may make the *P. oryzae* fungus less effective at infecting plants, reducing its ability to compete with sensitive strains in the field (Kimura and Fujimoto 2015; Mikaberidze and McDonald 2015).

Interestingly, only some cases observed the effect of chlorothalonil in controlling rice blast disease (Sultana

et al. 2020; Kafle *et al.* 2021) and used in combination with tricyclazole or azoxystrobin (LPAU&LPBU in Vietnam 2023). However, 33% of *P. oryzae* isolates in this study were medium resistant to chlorothalonil, though the EC50 was relatively low. Chlorothalonil is a broad-spectrum contact fungicide that inhibits spore germination and disrupts cellular respiration in fungal pathogens, including *P. oryzae*. This multisite action makes it difficult for the *P. oryzae* fungus to develop resistance, as multiple simultaneous genet (Brent 1995). As a contact fungicide, chlorothalonil remains on the plant's surface and does not penetrate the tissue, unlike systemic fungicides, and reduces the opportunity for *P. oryzae* to develop resistance (Kilian and Steiner 2003).

With the current level of chemical use, the emergence of resistant populations is inevitable. The search for alternatives to chemicals to control rice blast disease is ongoing. Innovations in nanoscience have revolutionized technology and there are promising applications of nano-silver pesticides that combat various phytopathogens with more efficient and lower application rates based on their outstanding antimicrobial activity (Wang *et al.* 2021). Previous studies reported that AgNPs were proven to control the *P. oryzae* fungus, causing rice blast disease. Mixing AgNPs with Trihexad 700 WP (containing 30 g · kg^{-1} hexaconazole and 670 g · kg^{-1} tricyclazole) significantly inhibited the mycelial growth of *P. oryzae* (Pham *et al.* 2018). Combining AgNPs with azoxystrobin at appropriate ratios enhanced fungitoxicity to azoxystrobin-sensitive/resistant *Magnaporthe oryzae* strains (Shi *et al.* 2023). Here, Ag/SiO_2 NCs can be used alone, since it effectively inhibits the *P. oryzae* mycelial growth with the low EC50 values of 17.14 μg · ml^{-1} (for TM4) and 19.04 μg · ml^{-1} (for TAT2). Moreover, silica, one of the ingredients in Ag/SiO_2 NCs, promotes rice growth, improves the morphology of rice plants during the reproductive period and reduces lodging, resulting in improved crop yield and qualitymin*al.* 2009; Khan *et al.* 2022). Moreover, Ag ions released from AgNPs under humid conditions can promote the formation of reactive oxygen species (ROS), which further damage cell structure, increase oxidative stress levels, induce cell death, and disrupt the transduction pathways (Fan *et al.* 2021). Therefore, Ag/SiO_2 NCs have enormously changed the hyphal structure of *P. oryzae* mycelium compared to chemical compounds. As a result, Ag/SiO_2 synthesized with participants of SiO_2 and CMC as a stabilizer presents a promising alternative to chemical treatments for managing rice blast disease and other plant pathogens. To increase the effectiveness of fungal disease control in practice, reduce the possibility of resistance formation of pathogens to chemicals, and increase the economic value of rice, the possibility of using Ag/SiO_2 alone or combined with a chemically active ingredient needs to be continuously investigated.

Conclusion

A total of 30 *P. oryzae* isolates were obtained from diseased samples collected across various locations in the Mekong Delta. The mycelium was thin, gray-white, with a clear margin around the fungal colony and melanin pigment in the colony's center. The conidia were a pyriform shape or shorter pyriform, containing two septa. All *P. oryzae* isolates were sensitive to tricyclazole; 67% were sensitive, and 33% were medium-sensitive to chlorothalonil; 17% of *P. oryzae* isolates were sensitive, 57% were medium-sensitive, 23% were resistant, and 3% were highly resistant to azoxystrobin. The Ag/SiO_2 nanocomposites were synthesized with the average size of AgNPs equal to 6.4 ± 0.1 nm. Ag/SiO_2 NCs inhibited the mycelium growth of *P. oryzae* isolates, causing the breaking of filaments and damage to fungal cell wall integrity. The properties of Ag/SiO_2 NCs include controlling particle size, changing stabilizers, and hybridizing, which could be improved, enabling Ag/SiO_2 to meet more requirements as to be an alternative solution for controlling rice blast disease caused by chemical-resistant *P. oryzae*.

Acknowledgements

The research was conducted with the financial support of the Nong Lam University Ho Chi Minh City (NLU) under Grant No CS-CB23-NH-01.

References

Abdel-Ghany T.M., Ganash M., Bakri M.M., Al-Rajhi A.M.H. 2018. Molecular characterization of *Trichoderma asperellum* and lignocellulolytic activity on barley straw treated with silver nanoparticles. BioResources 13 (1): 1729–1744. DOI: https://doi.org/10.15376/biores.13.1.1729-1744

Akter M., Sikder M.T., Rahman M.M., Ullah A.K.M.A., Hossain K.F.B., Banik S., Hosokawa T., Saito T., Kurasaki M. 2018. A systematic review on silver nanoparticles-induced cytotoxicity: Physicochemical properties and perspectives. Journal of Advanced Research 9: 1–16. DOI: https://doi.org/10.1016/j.jare.2017.10.008

Al-Zubaidi S., Al-Ayafi A., Abdelkader H. 2019. Biosynthesis, characterization and antifungal activity of silver nanoparticles by *Aspergillus niger* isolate. Journal of Nanotechnology Research 02 (2019): 22–35. DOI: https://doi.org/10.26502/jnr.2688-8521002

Baka Z.A., El-Zahed M.M. 2022. Antifungal activity of silver/silicon dioxide nanocomposite on the response of faba bean plants (*Vicia faba* L.) infected by *Botrytis cinerea*. Bioresources and Bioprocessing 9 (1): 102. DOI: https://doi.org/10.1186/s40643-022-00591-7

Balba H. 2007. Review of strobilurin fungicide chemicals. Journal of Environmental Science and Health, Part B 42 (4): 441–451. DOI: https://doi.org/10.1080/03601230701316465

Balouiri M., Sadiki M., Ibnsouda S.K. 2016. Methods for in vitro evaluating antimicrobial activity: A review. Journal of Pharmaceutical Analysis 6 (2): 71–79 DOI: https://doi.org/10.1016/j.jpha.2015.11.005

Bezerra G.A., Chaibub A.A., Oliveira M.I.S., Mizubuti E.S.G., Filippi M.C.C. 2021. Evidence of *Pyricularia oryzae* adaptability to tricyclazole. Journal of Environmental Science and Health, Part B 56 (10): 869–876. DOI: https://doi.org/10.1080/03601234.2021.1971913

Brent K.J. 1995. Fungicide resistance in crop pathogens: how can it be managed? FRAC Monograph no. 1. GIFAP, Brussels, 48 pp.

Cai M., Miao J., Chen F., Li B., Liu X. 2021. Survival Cost and Diverse Molecular Mechanisms of *Magnaporthe oryzae* Isolate Resistance to Epoxiconazole. Plant Disease 105 (2): 473–480. DOI: https://doi.org/10.1094/PDIS-02-20-0393-RE

Chuan-qing Z., Ming-gu Z., Zhen-run S., Gui-mei L. 2004. Detection of sensitivity and resistance variation of *magnaporthe grisea* to kitazin p, carbendazim and tricyclazole. Rice Science 11 (5): 317–326.

D'Ávila L.S., De Filippi M.C.C., Café-Filho A.C. 2021. Sensitivity of *Pyricularia oryzae* populations to fungicides over a 26-year time frame in Brazil. Plant Disease 105 (6): 1771–1780. DOI: https://doi.org/10.1094/PDIS-08-20-1806-RE

D'Ávila L.S., De Filippi M.C.C., Café-Filho A.C. 2022. Fungicide resistance in *Pyricularia oryzae* populations from southern and northern Brazil and evidence of fitness costs for QoI-resistant isolates. Crop Protection 153: 105887. DOI: https://doi.org/10.1016/j.cropro.2021.105887

Dorigan A.F., CarvalhoG.D., Poloni N.M., Negrisoli M.M., Maciel J.L.N., Ceresini P.C. 2019. Resistance to triazole fungicides in *Pyricularia* species associated with invasive plants from wheat fields in Brazil. Acta Scientiarum. Agronomy 41 (1): 39332. DOI: https://doi.org/10.4025/actasciagron.v41i1.39332

Fan X., Yahia L., Sacher E. 2021. Antimicrobial properties of the Ag, Cu nanoparticle system. Biology 10 (2): 137. DOI: https://doi.org/10.3390/biology10020137

Fang M., Yan L., Wang Z., Zhang D., Ma Z. 2009. Sensitivity of *Magnaporthe grisea* to the sterol demethylation inhibitor fungicide propiconazole. Journal of Phytopathology 157 (9): 568–572. DOI: https://doi.org/10.1111/j.1439-0434.2009.01576.x

FAOSTAT. 2024. Food and agriculture data. 2024. [Available on: https://www.fao.org/faostat/en/#data/QCL] [Accessed on: 24 August 2024]

Froyd J.D. 1978. Methods of applying tricyclazole for control of P*yricularia oryzae* on rice. Phytopathology 68 (5): 818. DOI: https://doi.org/10.1094/Phyto-68-818

Gouot J.M. 1988. Characteristics and population dynamics of *Botrytis cinerea* and other pathogens resistant to dicarboximides. p. 53–55 In: "Fungicide Resistance in North America" (C.J. Delp, ed.) American Phytopathological Society, St. Paul, MN, USA.

Guo B., Lou Y., Liang Y., Zhang J., Hua H., Xi Y. 2004. Effects of nitrogen and silicon applications on the growth and yield of rice and soil fertility. Chinese Journal of Ecology (6): 33–36.

Guo Z., Zeng G., Cui K., Chen A. 2019. Toxicity of environmental nanosilver: mechanism and assessment. Environmental Chemistry Letters 17 (1): 319–333. DOI: https://doi.org/10.1007/s10311-018-0800-1

Habash M.B., Park A.J., Vis E.C., Harris R.J., Khursigara C.M. 2014. Synergy of silver nanoparticles and aztreonam against *Pseudomonas aeruginosa* pao1 biofilms. Antimicrobial Agents and Chemotherapy 58 (10): 5818–5830. DOI: https://doi.org/10.1128/AAC.03170-14

Hirooka T., Ishii H. 2013. Chemical control of plant diseases. Journal of General Plant Pathology 79 (6): 390–401. DOI: https://doi.org/10.1007/s10327-013-0470-6

Kafle K., Poudel A., Manandhar S., Adhikari N. 2021. Efficacy of different fungicides against the in-vitro growth of Pyricularia oryzae causing Rice blast disease. International Journal of Environment, Agriculture and Biotechnology 6 (3):153–157. DOI https://doi.org/10.22161/ijeab.63.17

Karunakaran G., Suriyaprabha R., Manivasakan P., Yuvakkumar R., Rajendran V., Prabu P., Kannan N. 2013. Effect of nanosilica and silicon sources on plant growth promoting rhizobacteria, soil nutrients and maize seed germination. IET Nanobiotechnology 7 (3): 70–77. DOI: https://doi.org/10.1049/iet-nbt.2012.0048

Khan F., Pandey P., Upadhyay T.K. 2022. Applications of nanotechnology-based agrochemicals in food security and sustainable agriculture: an overview. Agriculture 12 (10): 1672. DOI: https://doi.org/10.3390/agriculture12101672

Kilian M., Steiner U. 2003. DISEASE | Bactericides and Fungicides. p. 190–198. In: "Encyclopedia of Rose Science" (Roberts, A.V., ed.). Elsevier, Oxford. DOI: https://doi.org/10.1016/B0-12-227620-5/00155-5

Kim K.J., Sung W.S., Suh B.K., Moon S.K., Choi J.S., Kim J.G., Lee D.G. 2008. Antifungal activity and mode of action of silver nano-particles on *Candida albicans*. BioMetals 22 (2): 235–242. DOI: https://doi.org/10.1007/s10534-008-9159-2

Kimura N., Fujimoto H. 2015. Fitness studies between field isolates of *Magnaporthe oryzae* resistant and sensitive to scytalone dehydratase inhibitors of melanin biosynthesis (MBIDs) and decline of frequency of resistant isolates at a rice field. Journal of Plant Diseases and Protection 122 (5/6): 224–228. DOI: https://doi.org/10.1007/BF03356556

Kunova A., Cortesi P. 2013. Tricyclazole and azoxystrobin in rice blast management : a review of thier activity ad pathogen responses. p. 39–66. In: "Fungicides: Classification, Role in Disease Management and Toxicity Effects" (Wheeler M.N., Johnston B.R., eds.). Nova Science Publishers, Inc.; New York, USA, 121 pp.

Kunova A., Pizzatti C., Bonaldi M., Cortesi P. 2014. Sensitivity of nonexposed and exposed populations of *Magnaporthe oryzae* from rice to tricyclazole and azoxystrobin. Plant Disease 98 (4): 512–518. DOI: https://doi.org/10.1094/PDIS-04-13-0432-RE

Liang Y., Nikolic M., Belanger R., Gong H., Song A. 2015. Effect of Silicon on Crop Growth, Yield and Quality. p. 209–223. In: "Silicon in Agriculture". Springer, Dordrecht. DOI: https://doi.org/10.1007/978-94-017-9978-2_11

Longya A., Talumphai S., Jantasuriyarat C. 2020. Morphological characterization and genetic diversity of rice blast fungus, *Pyricularia oryzae*, from thailand using issr and srap markers. Journal of Fungi 6 (1): 38. DOI: https://doi.org/10.3390/jof6010038

LPAU&LPBU in Vietnam. 2023. Revising List of Pesticides Approved for Use and the List of Pesticides Banned from Use in Vietnam. 2023] [Available on: https://datafiles.chinhphu.vn/cpp/files/vbpq/2023/11/09-bnn.signed.pdf. [Accessed on: 23 August 2024]

Mew T.-W., Gonzales P. 2002. A Handbook of Rice Seedborne Fungi. Los Bafios (Philippines): International Rice Research Institute, and Enfield, N.H. (USA): Science Publishers, Inc., 83 pp.

Mikaberidze A., McDonald B. 2015. Fitness Cost of Resistance: Impact on Management. p. 77–89. In: "Fungicide Resistance in Plant Pathogens. Principles and a Guide to Practical Management" (Ishii H., Hollomon D.W., eds.). Springer Japan, 490 pp. DOI: https://doi.org/10.1007/978-4-431-55642-8_6

Nalley L., Tsiboe F., Durand-Morat A., Shew A., Thoma G. 2016. Economic and Environmental Impact of Rice Blast Pathogen (*Magnaporthe oryzae*) Alleviation in the United

States. PLOS ONE 11 (12): e0167295. DOI: https://doi.org/10.1371/journal.pone.0167295

Navarro E., Baun A., Behra R., Hartmann N.B., Filser J., Miao A.J., Quigg A., Santschi P.H., Sigg L. 2008. Environmental behavior and ecotoxicity of engineered nanoparticles to algae, plants, and fungi. Ecotoxicology 17 (5): 372–386. DOI: https://doi.org/10.1007/s10646-008-0214-0

Nguyen H.C., Nguyen T.T., Dao T.H., Ngo Q.B., Pham H.L., Nguyen T.B.N. 2016. Preparation of Ag/SiO 2 nanocomposite and assessment of its antifungal effect on soybean plant (a Vietnamese species DT-26). Advances in Natural Sciences: Nanoscience and Nanotechnology.7 (4): 045014. DOI: https://doi.org/10.1088/2043-6262/7/4/045014

Okey-Onyesolu C.F., Hassanisaadi M., Bilal M., Barani M., Rahdar A., Iqbal J., Kyzas G.Z. 2021. Nanomaterials as nanofertilizers and nanopesticides: an overview. ChemistrySelect 6 (33): 8645–8663. DOI: https://doi.org/10.1002/slct.202102379

Park S.Y., Han K., O'Neill D.B., Mul G. 2017. Stability of Ag@ SiO 2 core-shell particles in conditions of photocatalytic overall water-splitting. Journal of Energy Chemistry 26 (2): 309–314. DOI: https://doi.org/10.1016/j.jechem.2016.12.010

Pham D.C., Nguyen T.H., Ngoc U.T.P., Le N.T.T., Tran T.V., Nguyen D.H. 2018. Preparation, characterization and antifungal properties of chitosan-silver nanoparticles synergize fungicide against *Pyricularia oryzae*. Journal of Nanoscience and Nanotechnology 18 (8): 5299–5305. DOI: https://doi.org/10.1166/jnn.2018.15400

Pham N.B.T., Le V.K.T., Bui T.T.T., Phan N.G.L., Tran Q.V., Nguyen M.L., Dang V.Q., Nguyen T.T., Vo T.N.H., Tran C.K. 2021. Improved synthesis of Ag/SiO_2 colloidal nanocomposites and their antibacterial activity against *ralstonia solanacearum* 15. Journal of Nanoscience and Nanotechnology 21 (3): 1598–1605. DOI: https://doi.org/10.1166/jnn.2021.19021

Prema P., Thangapandiyan S., Immanuel G. 2017. CMC stabilized nano silver synthesis, characterization and its antibacterial and synergistic effect with broad spectrum antibiotics. Carbohydrate Polymers 158: 141–148. DOI: https://doi.org/10.1016/j.carbpol.2016.11.083

Rangelova N., Aleksandrov L., Angelova T., Georgieva N., Müller R. 2014. Preparation and characterization of SiO2/CMC/Ag hybrids with antibacterial properties. Carbohydrate Polymers 101: 1166–1175. DOI: https://doi.org/10.1016/j.carbpol.2013.10.041

Salem S.S., Hashem A.H., Sallam A.-A.M., Doghish A.S., Al--Askar A.A., Arishi A.A., Shehabeldine A.M. 2022. Synthesis of silver nanocomposite based on carboxymethyl cellulose: antibacterial, antifungal and anticancer activities. Polymers 14 (16): 3352. DOI: https://doi.org/10.3390/polym14163352

Shi H., Wen H., Xie S., Li Y., Chen Y., Liu Z., Jiang N., Qiu J., Zhu X., Lin F. and Kou Y. 2023. Antifungal activity and mechanisms of AgNPs and their combination with azoxystrobin against *Magnaporthe oryzae*. Environmental Science: Nano 10 (9): 2412–2426. DOI: https://doi.org/10.1039/D3EN00168G

Song J.J., Soytong K., Kanokmedhakul S. 2022. Control of rice blast disease caused by *Magnaporthe oryzae* by application of antifungal nanomaterials from *Emericella nidulans*. Plant Protection Science 58 (1): 40–48. DOI: http://doi.org/10.17221/33/2021-PPS

Sultana R., Zohura F., Rahman M., Hasan A., Meah M., Hossain M. 2020. Evaluation of some fungicides in controlling blast of rice var. Kalijira in Mymensingh. Journal of Bangladesh Agricultural University (0): 1. DOI: https://doi.org/10.5455/JBAU.136288

Tran N.T., Dat H, Pham L. H. , Vo T.V, Nguyen N.N., Tran C.K., Nguyen D.M., Nguyen T.T.T., Tran T.T.V., Nguyen P.L.M., Hoang D.Q. 2023. Ag/SiO2 nanoparticles stabilization with lignin derived from rice husk for antifungal and antibacterial activities. International Journal of Biological Macromolecules 230: 123124. DOI: https://doi.org/10.1016/j.ijbiomac.2022.123124

Wang Y., Deng C., Rawat S., Cota-Ruiz K., Medina-Velo I., Gardea-Torresdey J.L. 2021. Evaluation of the effects of nanomaterials on rice (O*ryza sativa* l.) responses: underlining the benefits of nanotechnology for agricultural applications. ACS Agricultural Science & Technology 1 (2): 44–54. DOI: https://doi.org/10.1021/acsagscitech.1c00030

Woloshuk C.P., Sisler H.D., Tokousbalides M.C., Dutky S.R. 1980. Melanin biosynthesis in *Pyricularia oryzae*: Site of tricyclazole inhibition and pathogenicity of melanin-deficient mutants. Pesticide Biochemistry and Physiology 14 (3): 256–264. DOI: https://doi.org/10.1016/0048-3575(80)90032-2

Wiraswati S. M., Iman R., Abdjad A.N., Wahyudi A.T. 2019. Antifungal activities of bacteria producing bioactive compounds isolated from rice phyllosphere against *Pyricularia oryzae*. Journal of Plant Protection Research 59 (1): 86–94. DOI: https://doi.org/10.24425/jppr.2019.126047